# Nuclear magnetic relaxation in the Ising-like antiferromagnet $CsCoCl_3$: Domain-wall pairing in the 3D ordered phase

T. Kohmoto
*Department of Physics, Faculty of Science, Kobe University, Nada-ku, Kobe 657, Japan*

T. Goto, S. Maegawa, and N. Fujiwara
*Graduate School of Human and Environmental Studies, Kyoto University, Sakyo-ku, Kyoto 606, Japan*

Y. Fukuda and M. Kunitomo
*Department of Physics, Faculty of Science, Kobe University, Nada-ku, Kobe 657, Japan*

M. Mekata
*Department of Applied Physics, Faculty of Engineering, Fukui University, Bunkyo, Fukui 910, Japan*
(Received 6 July 1993)

The longitudinal relaxation time $T_1$ and the transverse relaxation time $T_2$ of $^{133}Cs$ NMR were measured in the three-dimensional ordered phase of a quasi-one-dimensional $S=\frac{1}{2}$ Ising-like antiferromagnet $CsCoCl_3$. The experimental results were well explained by a pulselike fluctuation due to spin inversion in the $Co^{2+}$ chains. This fact strongly suggests the presence of domain-wall pairing in the linear chain. The spin-inversion rate, the spin-inversion duration, and the correlation time were evaluated from an analysis of fluctuating internal field at the Cs nuclei. The mechanism of the phase transition at $T_{N2}$ (9 K) was made clear from the dynamical point of view.

## I. INTRODUCTION

The magnetic linear chain on the triangular lattice is known to exhibit attractive behaviors both from the static and the dynamic points of view. The hexagonal compound $CsCoCl_3$ is a typical example of quasi-one-dimensional $S=\frac{1}{2}$ Ising-like antiferromagnets on the triangular lattice,[1] and a great deal of work has been devoted to the study of this compound experimentally[2-14] and theoretically.[15-24] This compound is characterized by successive phase transitions, which occur at $T_{N1}=21$ K and $T_{N2}=9$ K.[3] The successive phase transitions have been explained by the spin frustration effect on the triangular-lattice antiferromagnet.[16] The intermediate phase between $T_{N1}$ and $T_{N2}$ is a partially disordered phase, where two-thirds of the magnetic chains order antiferromagnetically with each other leaving the rest uncorrelated. The low-temperature phase below $T_{N2}$ is a ferrimagnetic phase, where all magnetic chains order in a collinear ferrimagnetic arrangement.

The dynamical behavior in the Ising-like linear chain can be described by the domain-wall picture, and the propagation of domain-wall soliton[15] is expected in the intermediate ($T_{N2}<T<T_{N1}$) and the paramagnetic ($T_{N1}<T$) phases. The existence of the propagating soliton in the $Co^{2+}$ chain in those phases has been established by the neutron-scattering,[4,6] electron-spin-resonance (ESR),[7-9] nuclear-magnetic-resonance (NMR),[11] and optical[14] experiments.

The propagation of domain-wall soliton has been discussed in the intermediate and the paramagnetic phases. However, the ESR signal due to domain walls was observed not only in the intermediate phase but also in the three dimensionally (3D) ordered phase below $T_{N2}$ (low-temperature phase).[7] The existence of domain walls suggests some nonlinear excitation remain even in the low-temperature phase, although the information on the detailed dynamics is not obtained from the ESR experiment. The possibility of the soliton propagation in one-third of the chains in the low-temperature phase was discussed in the experiment of the temperature dependence of $^{133}Cs$ NMR spectrum.[12] The propagation of free domain walls (solitons) in the 3D ordered phase is not plausible. However, it is very interesting that the domain walls may propagate in some form in the 3D ordered low-temperature phase. Recently, pair states and bound states of solitons in $CsCoCl_3$ and $CsCoBr_3$ were discussed theoretically.[23,24] In the Heisenberg antiferromagnet $(CH_3)_4NMnCl_3$ (TMMC), where sine-Gordon type of soliton propagates in the magnetic chain above $T_N$, the pairing of solitons below $T_N$ has been discussed theoretically[25,26] and experimentally.[27]

In this paper we pay attention to the dynamical behavior of the $Co^{2+}$ spins in the low-temperature phase. In order to make the spin dynamics clear, we measured the longitudinal relaxation time $T_1$ and the transverse relaxation time $T_2$ of $^{133}Cs$ NMR in the low-temperature phase of $CsCoCl_3$. The observed values of $T_1$ and $T_2$ exhibited characteristic dependences on the temperature, the NMR line, and the NMR frequency. From an analysis of fluctuating internal field, we found the presence of a pulselike fluctuation of the local field at the Cs nuclei, whose pulse width is of the order of $10^{-6}$ sec. The analysis of $T_2$ has already been reported in the previous

 

paper.[28] In the present paper we report on the detailed results of the statistical properties of the pulselike fluctuation obtained consistently from the analyses of $T_1$ and $T_2$. This pulselike fluctuation suggests that the domain walls move in the form of a pair in the $Co^{2+}$ chain, which results in a short-time spin inversion away from the stable spin directions in the linear chain. The other techniques such as the ESR and the neutron scattering have not given any direct information on the domain-wall pairing in $CsCoCl_3$.

The pulsed-NMR method is one of the powerful techniques for the study of the spin dynamics in magnetic systems. The dynamical behavior of the electron spin can be probed through the relaxation times of the nuclear spin near the electron spin. The analyses of the longitudinal relaxation time $T_1$ and the transverse relaxation time $T_2$ individually give useful information on the local-field fluctuation from different points of view. When the results on $T_1$ and $T_2$ are interpreted consistently by a model, the information can be much improved both in quality and quantity.

We analyzed the experimental results at first by using the conventional stochastic theory of relaxation.[29–32] The result on $T_1$ was found to be well explained by the stochastic theory. The result on $T_2$, on the other hand, was difficult to be explained. One of the reasons is probably that the conventional stochastic theory of relaxation is valid only for the case of weak collision and is not necessarily applicable to general cases. In order to explain our experimental result on $T_2$, we developed a nonlinear theory of phase relaxation in a pulse fluctuating field valid for general cases including both the weak- and strong-collision limits. By using our theory the experimental results on $T_2$ was well explained by a pulselike fluctuating field. The statistical properties of the pulselike fluctuation were determined by consistent interpretation of the experimental results on $T_1$ and $T_2$.

## II. EXPERIMENT OF $^{133}$Cs NMR

The hexagonal $CsCoCl_3$ is known to be a good realization of Ising antiferromagnetic linear chain. Assuming the chain axis to be along the $z$-axis, the intrachain Hamiltonian is written as

$$\mathcal{H}=-2J\sum_j\{S_j^zS_{j+1}^z+\varepsilon(S_j^xS_{j+1}^x+S_j^yS_{j+1}^y)\}\ , \qquad (1)$$

where $S=\frac{1}{2}$, $J=-75$ K, and $\varepsilon\simeq 0.14$.[2,4] The nearest-neighbor interchain interaction $J_1$ is antiferromagnetic and is much weaker than the intrachain interaction ($J_1\sim 10^{-2}J$)[18]

In the low-temperature phase, the electron spins of the $Co^{2+}$ ion in the linear chain are ordered antiferromagnetically, and the $Co^{2+}$ chains on the triangular lattice take a collinear ferrimagnetic arrangement in the $c$ plane as shown in Fig. 1(a). The Cs nucleus is located in the center of the six $Co^{2+}$ ions, which form a triangular prism with a threefold axis along the $c$ axis. The internal field $\mathbf{h}_0$ ($h_0\sim 0.43$ kOe) at the Cs nucleus is due to the dipolar interactions with the surrounding $Co^{2+}$ magnetic moments, and its direction lies in the $c$ plane.[10] There are six magnetically nonequivalent Cs sites, where the directions of the internal field are different in the $c$ plane as is seen in Fig. 1(b). Three of them are shown by the arrows in Fig. 1(a). The others appear in other domains of the ferrimagnetic structure.

In the presence of an external field $\mathbf{H}_0$, the total magnetic field at each Cs site is determined by the vector sum of $\mathbf{H}_0$ and $\mathbf{h}_0$. When the external field is applied in the $c$ plane and its magnitude is swept with the operating frequency fixed, six NMR lines at most can appear corresponding to the different directions of the internal field. Three NMR lines, which we refer to as $a_1$-$a_3$ lines, appear in the external field parallel to the $a$ axis as shown in Fig. 1(c), and four lines, which we refer to as $b_1$-$b_4$ lines, appear in the external field perpendicular to the $a$ axis as shown in Fig. 1(d). The values of $T_1$ and $T_2$ were measured for these seven lines.

The experiment was made by using a coherent pulsed-NMR spectrometer equipped with a personal computer for the pulse-sequence control and the signal processing. The longitudinal relaxation time $T_1$ and the transverse relaxation time $T_2$ were measured at the resonance frequency $\omega/2\pi=1.5$–$6.7$ MHz ($H_0=2$–$12$ kOe) in the temperature range between 4.2 and 7.5 K. The value of $T_1$ was determined by observing the recovery of the spin-echo signal after the saturation by a comb of rf pulses. The value of $T_2$ was determined by observing the decay of the spin-echo signal as a function of the time separation of the two rf pulses.

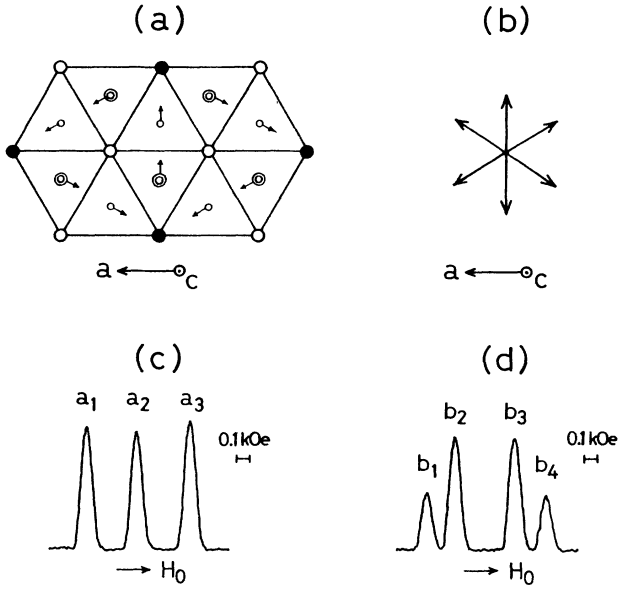


FIG. 1. (a) Ferrimagnetic structure of the $Co^{2+}$ spins in the $c$ plane in the low-temperature phase ($T<T_{N2}$). The $Co^{2+}$ spins are represented by ○ (up for $z=0$, down for $z=\frac{1}{2}$) and ● (down for $z=0$, up for $z=\frac{1}{2}$). The $^{133}$Cs nuclei are represented by ∘ ($z=\frac{1}{4}$) and ◎ ($z=\frac{3}{4}$). (b) Six directions of the internal fields ($h_0\sim 0.43$ kOe, in the $c$ plane) at the six Cs sites. Three of them are shown by the arrows in (a). The others appear in other domains of the ferrimagnetic structure. (c) NMR spectrum observed in $\mathbf{H}_0\|\mathbf{a}$ axis. (d) NMR spectrum observed in $\mathbf{H}_0\perp\mathbf{a}$ axis.

### III. EXPERIMENTAL RESULTS

The temperature dependences of $1/T_1$ at $\omega/2\pi=5.0$ MHz for the $a_1$, $a_2$, $b_1$, and $b_2$ lines are shown in Fig. 2. The values of $1/T_1$ for the $a_3$, $b_3$, and $b_4$ lines are the same as those for the $a_1$, $b_2$, and $b_1$ lines, respectively, within the experimental error. Near the temperature $T_{N2}$ the measurements of $T_1$ and $T_2$ values were not easy because the transverse relaxation time $T_2$ becomes very short and the signal intensity of the spin echoes becomes very small. Figure 3 shows the temperature dependences of $1/T_1$ for the $a_1$ line at $\omega/2\pi=3.0$, 5.0, and 6.7 MHz. Those for the other lines show similar frequency dependencies to those for the $a_1$ line in Fig. 3. The value of $1/T_1$ exhibits a remarkable increase with increasing temperature, and the temperature dependence is well described by the relation $1/T_1 \propto \exp(-|J|/kT)$ for all lines and frequencies; the solid lines in Figs. 2 and 3 represent the fitting lines obtained from the above relation.

The angular dependences of $1/T_1$ at the temperature $T=5.7$ K and at $\omega/2\pi=2.0$, 3.0, 5.0, and 6.7 MHz are shown in Fig. 4. The seven data for a fixed frequency are the measured values of $1/T_1$ for the seven NMR lines, the $a_1$-$a_3$ lines in Fig. 1(c) and the $b_1$-$b_4$ lines in Fig. 1(d). Here $\theta$ represents the angle between the directions of the external field $\mathbf{H}_0$ and the internal field $\mathbf{h}_0$ at the Cs site. Since $H_0 \gg h_0$ in our experimental condition, $|\mathbf{H}_0+\mathbf{h}_0| \simeq H_0+h_0\cos\theta$. The values of $\theta$ corresponding to the $a_1$, $a_2$, $a_3$, $b_1$, $b_2$, $b_3$, and $b_4$ lines are 30°, 90°, 150°, 0°, 60°, 120°, and 180°, respectively.

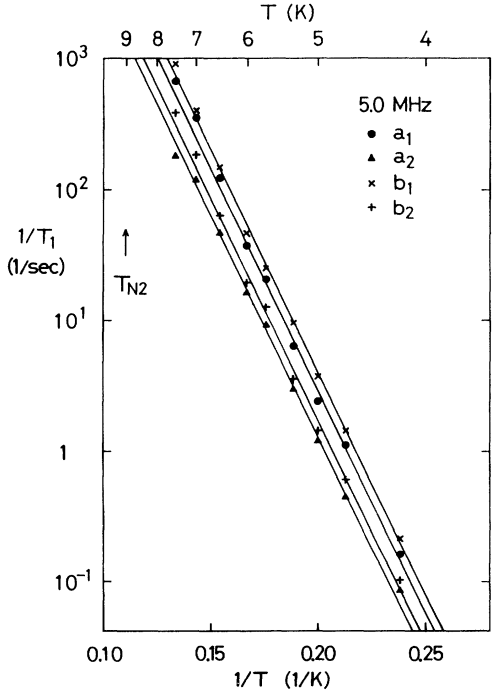


FIG. 2. Temperature dependences of $1/T_1$ at $\omega/2\pi=5.0$ MHz for the $a_1$, $a_2$, $b_1$, and $b_2$ lines. The values of $1/T_1$ for the $a_3$, $b_3$, and $b_4$ lines are the same as those for the $a_1$, $b_2$, and $b_1$ lines, respectively, within the experimental error. The solid lines represent the fitting lines obtained from the relation $1/T_1 \propto \exp(-|J|/kT)$.

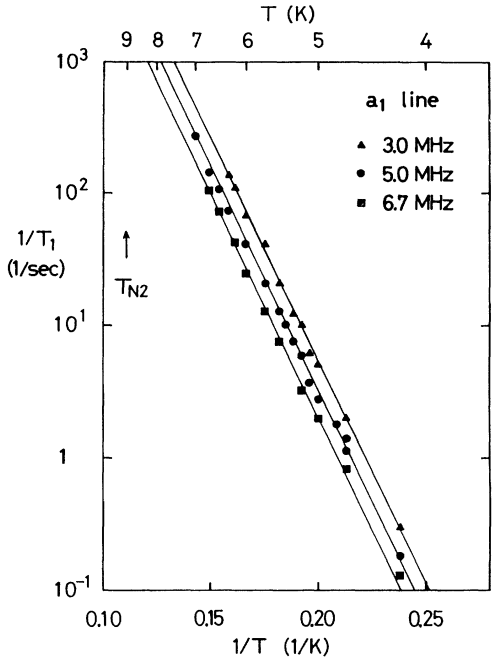


FIG. 3. Temperature dependences of $1/T_1$ for the $a_1$ line at $\omega/2\pi=3.0$, 5.0, and 6.7 MHz. Those for the other lines show similar frequency dependencies to those for the $a_1$ line. The solid lines represent the fitting lines obtained from the relation $1/T_1 \propto \exp(-|J|/kT)$.

The temperature dependences of $1/T_2$ for the $a_1$, $a_2$, $b_1$, and $b_2$ lines are shown in Fig. 5. The value of $1/T_2$ for the $a_3$, $b_3$, and $b_4$ lines are the same as those for the $a_1$, $b_2$, and $b_1$ lines, respectively. Figure 6 shows the angular dependence of $1/T_2$ at $T=5.7$ K and at

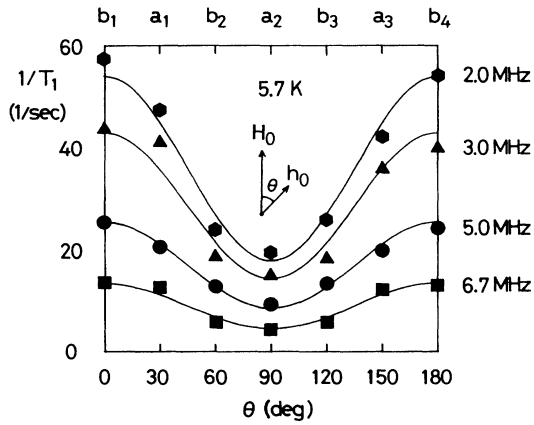


FIG. 4. Angular dependences of $1/T_1$ at $T=5.7$ K and at $\omega/2\pi=2.0$, 3.0, 5.0, and 6.7 MHz. $\theta$ represents the angle between the directions of the external field $\mathbf{H}_0$ and the internal field $\mathbf{h}_0$ at the Cs site. The seven data for a fixed frequency are the measured values of $1/T_1$ for the seven NMR lines [$a_1$-$a_3$ in Fig. 1(c) and $b_1$-$b_4$ in Fig. 1(d)]. The solid line is the theoretical curve obtained from the best fit of Eq. (26) to the measured values of $1/T_1$.

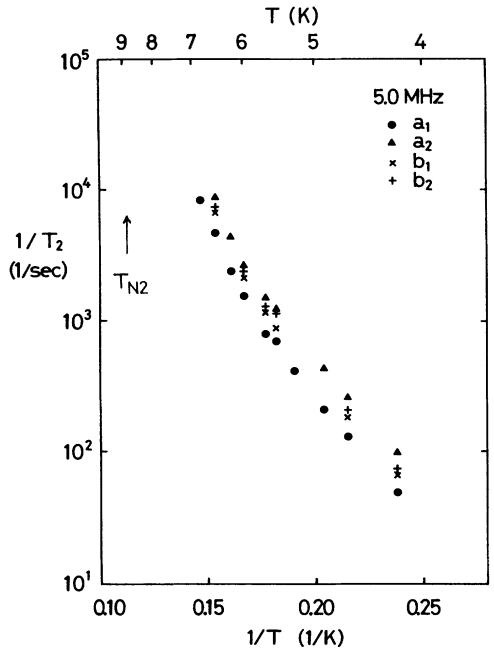


FIG. 5. Temperature dependences of $1/T_2$ at $\omega/2\pi=5.0$ MHz for the $a_1$, $a_2$, $b_1$, and $b_2$ lines. The values of $1/T_2$ for the $a_3$, $b_3$, and $b_4$ lines are the same as those for the $a_1$, $b_2$, and $b_1$ lines, respectively, within the experimental error.

$\omega/2\pi=5.0$ MHz. The seven dots are the measured values of $1/T_2$ for the seven NMR lines. The value of $1/T_2$ also exhibits a remarkable increase with increasing temperature, but does not exhibit appreciable frequency dependence; the same value of $T_2$ was obtained for each line in our frequency range, from 1.5 to 6.7 MHz, within the experimental error. It is interesting that the value of $1/T_1$ depends on the NMR frequency $\omega$ but the value of $1/T_2$ does not. This suggests the presence of a local-field fluctuation whose characteristic time is of the order of $1/\omega$.

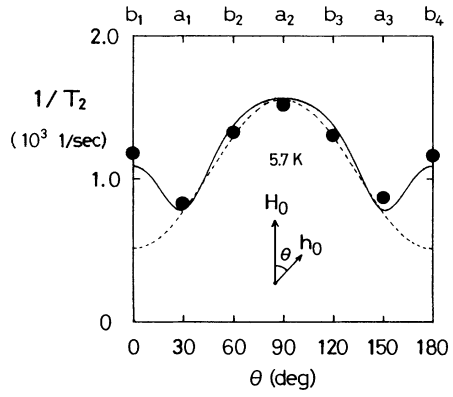


FIG. 6. Angular dependence of $1/T_2$ at $T=5.7$ K and at $\omega/2\pi=5.0$ MHz. $\theta$ represents the angle between the directions of the external field $\mathbf{H}_0$ and the internal field $\mathbf{h}_0$. The seven dots are the measured value of $1/T_2$ for the seven NMR lines [$a_1$-$a_3$ in Fig. 1(c) and $b_1$-$b_4$ in Fig. 1(d)]. The value of $1/T_2$ does not exhibit appreciable frequency dependence in our frequency range. The broken line is the theoretical curve expected from Eq. (15), the result of the conventional stochastic theory. The solid line is the theoretical curve obtained from the best fit of Eq. (23), the result of our nonlinear theory, to the measured values of $1/T_2$. The fitting parameters are $\tau_0=5.0\times10^{-4}$ sec and $\tau_1=1.6\times10^{-6}$ sec.

As is seen in Figs. 4 and 6, $1/T_1$ and $1/T_2$ at $T=5.7$ K exhibit characteristic angular ($\theta$) dependences. The value of $1/T_1$ takes the minimum value for $\theta=90°$ and the maximum value for $\theta=0°$ and 180°, and the latter is about three times as much as the former. The value of $1/T_2$, on the other hand, takes the minimum value for $\theta=30°$ and 150° and the maximum value for $\theta=90°$, and the latter is about twice as much as the former. Similar angular dependences were observed at the other temperatures as is seen in Figs. 2 and 5, although the values of $1/T_1$ and $1/T_2$ exhibited remarkable temperature dependences.

## IV. ANALYSIS BY THE STOCHASTIC THEORY

In this section we consider the stochastic theory of relaxation, which is the standard theory for the spin relaxation in the fluctuating local field. In the conventional stochastic theory, the fluctuation is assumed to be of the Gaussian process[29,30] or is treated as a perturbation.[31,32] Here we try to analyze our experimental results by using the stochastic theory, although the validity of the assumption is not obvious in our case, especially in the case of the transverse relaxation.

### A. Stochastic theory of relaxation

According to the conventional stochastic theory of relaxation,[29–32] the relaxation rates are described by using the time-correlation functions for the fluctuating field. Under the assumptions that the fluctuation is of a Gaussian process and the correlation function is of an exponential type, general expression of the transverse relaxation function can be derived analytically.[29,30] For a time much shorter than the correlation time $\tau_c$ for the fluctuation (short-time approximation), the decay curve is the Gaussian type. For a time much longer than $\tau_c$ (long-time approximation), on the other hand, the decay curve is the Lorentzian (exponential) type. Even in the case without the assumption of Gaussian process, the longitudinal and the transverse relaxation rates can be calculated for the long-time approximation (weak-collision limit) by using the perturbation theory, and are given by the Fourier transform of the correlation function for the fluctuating field.[31,32] For the long-time approximation, the results of the two treatments, of course, are the same.

In the case of long-time approximation, the longitudinal relaxation rate $\Gamma_1$ and the transverse relaxation rate $\Gamma_2$ are given by the spectral density $G_\alpha(\omega)$ of the longitudinal ($\alpha=z$) and transverse ($\alpha=\perp$) components of the fluctuating local field;

$$\Gamma_1=\frac{1}{T_1}=G_\perp(\omega)\ , \tag{2}$$

$$\Gamma_2=\frac{1}{T_2}=G_z(0)+\frac{1}{2}G_\perp(\omega)\ , \tag{3}$$

with

$$G_\alpha(\omega)=\frac{\gamma^2}{2}\int_{-\infty}^{+\infty}\langle \delta H_\alpha(t)\delta H_\alpha(0)\rangle \exp(i\omega t)dt \ , \quad (4)$$

where $\gamma$ is the gyromagnetic ratio, and $\delta H_z(t)$ and $\delta H_\perp(t)$ represent the longitudinal and transverse components of the fluctuating local field, respectively. The transverse relaxation rate $\Gamma_2$ is determined by the low-frequency component $G_z(0)$ in the Fourier spectrum of the longitudinal fluctuation and the $\omega$ component $G_\perp(\omega)$ in that of the transverse fluctuation, while the longitudinal relaxation rate $\Gamma_1$ is determined only by the $\omega$ component $G_\perp(\omega)$.

If the dominant contribution to the transverse relaxation rate is the $\omega$ component $G_\perp(\omega)$, the two rates $\Gamma_1$ and $\Gamma_2$ should be of the same order of magnitude. In our experiment, however, $\Gamma_2$ is much larger than $\Gamma_1$ ($\Gamma_2/\Gamma_1=T_1/T_2\sim 10^3$). Therefore, the dominant contribution to the transverse relaxation rate is the low-frequency component $G_z(0)$. In the following, we consider that the $\omega$ component $G_\perp(\omega)$ in the Fourier spectrum of the transverse fluctuation determines $\Gamma_1$ and the low-frequency component $G_z(0)$ in that of the longitudinal fluctuation determines $\Gamma_2$. Since $H_0 \gg h_0$ in our experiment, the direction of the external field can be taken as the quantization axis which is referred to as the $z$ axis.

If we assume an exponential type of the correlation functions,

$$\langle \delta H_\alpha(t)\delta H_\alpha(0)\rangle=(\Delta_\alpha)^2\exp\left[-\frac{|t|}{\tau_c}\right] , \quad (5)$$

where $(\Delta_\alpha)^2=\langle(\delta H_\alpha)^2\rangle$, and $\tau_c$ is the correlation time of the fluctuating field, then the expressions of $\Gamma_1$ and $\Gamma_2$ can be calculated easily from Eqs. (2)–(5);

$$\Gamma_1^s=(\gamma\Delta_\perp)^2\frac{\tau_c}{1+(\omega\tau_c)^2} , \quad (6)$$

$$\Gamma_2^s=(\gamma\Delta_z)^2\tau_c . \quad (7)$$

The relaxation rates are determined by those statistical parameters, the amplitude $\Delta_\alpha$ and the correlation time $\tau_c$ of the fluctuation.

### B. Correlation time

The result of the stochastic theory suggests that the correlation time $\tau_c$ may be obtained from the frequency dependence of the longitudinal relaxation rate. As is seen in Eq. (6), the characteristic of the frequency dependence of $\Gamma_1$ is determined by the dimensionless value of $\omega\tau_c$:

$$\Gamma_1^s\propto\frac{\tau_c}{1+(\omega\tau_c)^2}\simeq\begin{cases}1/(\omega^2\tau_c) & (\omega\tau_c\gg 1)\\ \tau_c & (\omega\tau_c\ll 1) .\end{cases} \quad (8)$$

In the case of $\omega\tau_c\gg 1$, the longitudinal relaxation rate is proportional to $(1/\omega)^2$. In the case of $\omega\tau_c\ll 1$, on the other hand, the rate is independent of $\omega$.

In our experiment, the value of $1/T_1$ depends on the NMR frequency $\omega$ as is seen in Figs. 3 and 4. The correlation time of the fluctuating field may be obtained from the $\omega$ dependence of $1/T_1$. Figure 7 shows the observed values of $1/T_1$ at $T=5.7$ K for the $a_1$ and $a_2$ lines for several values of frequency, $\omega/2\pi=1.5$–$6.7$ MHz. Similar frequency dependences were observed for the other lines as is seen in Fig. 4. This experimental result indicates that our case is not the limiting case and the value of $\omega\tau_c$ is of the order of unity in our frequency range. The solid lines in Fig. 7 represent the theoretical curves obtained from Eq. (6). The fitting value of the correlation time is $\tau_c=4\times10^{-8}$ sec.

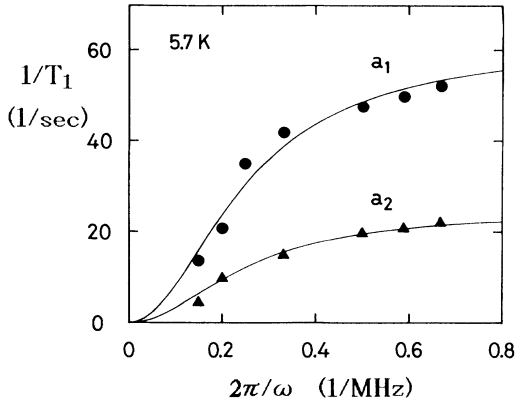


FIG. 7. Frequency dependences of $1/T_1$ at $T=5.7$ K for the $a_1$ and $a_2$ lines. Similar frequency dependences were observed for the other lines. The solid line is the theoretical curve obtained from the best fit of Eq. (6) or (26) to the measured values of $1/T_1$. The fitting value of the correlation time is $\tau_c=4\times10^{-8}$ sec.

Similar frequency dependences of $1/T_1$ were observed in the other temperatures, although the value of $1/T_1$ exhibited a remarkable temperature dependence. This fact indicates that the value of $\tau_c$ does not exhibit an appreciable change in our temperature range and

$$\tau_c\simeq 4\times10^{-8} \text{ sec} . \quad (9)$$

Since the value of $T_1$ is much longer than $\tau_c$, the long-time approximation for the longitudinal relaxation of Eqs. (2) and (4) is satisfied in our case.

### C. Spin-inversion model

As is seen in Figs. 3–7, the experimental results show interesting behaviors; the characteristic angular dependences in $1/T_1$ and $1/T_2$, the frequency dependence in $1/T_1$, and the frequency independence in $1/T_2$. These facts give important information on the statistical properties of fluctuating internal field at the Cs nuclei, which reflects the dynamical behavior of the electron spin in the linear chain.

In order to explain the above experimental results, we consider a spin-inversion model; the $Co^{2+}$ spins are inverted locally in the linear chain for a short time away from the stable directions, which are determined by the ferrimagnetic structure in the $c$ plane. It is expected that the spin inversion may occur in either of the two [open circles in Fig. 1(a)] of the three chains on the triangular lattice because it has no energy loss due to the interchain

interactions with six nearest-neighbor chains. Let us suppose that the spin inversion occurs in one linear chain. Then, the direction of the internal field rotates by $\pm 60°$ in the $c$ plane as shown in Fig. 8. Taking account of the Ising-like exchange interaction in $CsCoCl_3$, we can consider that the rotation occurs instantaneously.

Such a spin inversion may explain the characteristic angular dependence of $1/T_1$ and $1/T_2$ because the amplitude $\Delta_\alpha$ of the fluctuating field has the maximum value in the direction perpendicular to the stable direction of the internal field. Then the value of $1/T_1$ $(1/T_2)$ is expected to have the maximum value at $\theta=0°$ and $180°$ $(\theta=90°)$, since it is determined by the transverse component $\Delta_\perp$ (the longitudinal component $\Delta_z$).

The fluctuating field at the Cs nucleus due to one $Co^{2+}$ chain is considered to be a two-state pulse type of fluctuation as shown in Fig. 9(a). The component $\delta H_\alpha(t)$ of the field fluctuation is described by random sudden jumps between two field values with the magnitude $h_\alpha$ of the field jump. We assume a Markov process for the fluctuation; the internal field jumps back and forth between the stable direction with lifetime $\tau_0$ and the unstable direction with lifetime $\tau_1$. We also assume $\tau_0 \gg \tau_1$, since the direction of the internal field is stable in the three-dimensionally ordered phase.

The correlation function of the two-state pulse fluctuation can be calculated analytically and expressed by an exponential type of function.[33] The amplitude and the correlation time in Eq. (5) are given by

$$(\Delta_\alpha)^2=\frac{\tau_0\tau_1}{(\tau_0+\tau_1)^2}(h_\alpha)^2\simeq\frac{\tau_1}{\tau_0}(h_\alpha)^2 , \tag{10}$$

$$\tau_c=\frac{\tau_0\tau_1}{\tau_0+\tau_1}\simeq\tau_1 . \tag{11}$$

The approximation holds in the case of $\tau_0 \gg \tau_1$, and then the correlation time is equal to the shorter lifetime. The relaxation rates due to the fluctuating field in Fig. 9(a) are obtained from Eqs. (6), (7), (10), and (11);

$$\Gamma_1^s(h_\perp)=\frac{1}{\tau_0}\frac{(\gamma h_\perp\tau_1)^2}{1+(\omega\tau_1)^2} , \tag{12}$$

$$\Gamma_2^s(h_z)=\frac{1}{\tau_0}(\gamma h_z\tau_1)^2 . \tag{13}$$

These rates correspond to the contribution from the fluctuating field caused by the spin inversion in one $Co^{2+}$ chain near the Cs nucleus. The value of $h_\alpha$ depends on the angle $\theta$. In our case two dominant contributions are expected from the two chains.

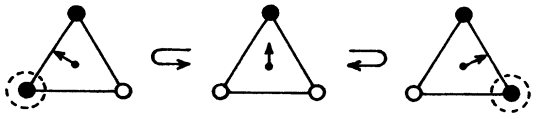

FIG. 8. Rotation of the internal field in the $c$ plane at the Cs site when the spin inversion occurs in one of the $Co^{2+}$ chains on the triangular lattice.

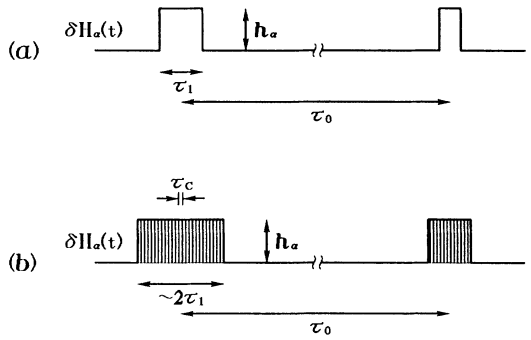


FIG. 9. Pulse fluctuating field $\delta H_\alpha(t)$ $(\alpha=z,\perp)$ at the Cs site due to the spin inversion in one $Co^{2+}$ chain near the Cs nucleus. (a) Simple pulse fluctuation with the magnitude $h_\alpha$ of the field jump and lifetimes $\tau_0$ and $\tau_1$. (b) Pulselike fluctuation with a temporal structure of the order of $\tau_c$ in a pulse.

### D. Analysis of the angular dependences

In this section we shall analyze the angular dependences of $1/T_1$ and $1/T_2$ in Figs. 4 and 6 by using the result of the stochastic theory on the basis of the pulse fluctuation expected from the rotation of the internal field.

According to the spin inversion model, there are two kinds of pulse fluctuations whose field jumps are $h_\alpha^\pm$ corresponding to the $\pm 60°$ rotations. We assume that the $\pm 60°$ rotations or the spin inversions in the two chains occur in equal probability. The relaxation rates are given by the sum of these two contributions:

$$\frac{1}{T_1}=\frac{1}{2}\{\Gamma_1^s(h_\perp^+)+\Gamma_1^s(h_\perp^-)\}$$
$$=\frac{1}{2\tau_0}\frac{(\gamma\tau_1)^2}{1+(\omega\tau_1)^2}\{(h_\perp^+)^2+(h_\perp^-)^2\} , \tag{14}$$

$$\frac{1}{T_2}=\frac{1}{2}\{\Gamma_2^s(h_z^+)+\Gamma_2^s(h_z^-)\}$$
$$=\frac{1}{2\tau_0}(\gamma\tau_1)^2\{(h_z^+)^2+(h_z^-)^2\} , \tag{15}$$

where $1/\tau_0$ is the fluctuation pulse rate at the Cs site, and then the spin-inversion rate in each of the two $Co^{2+}$ chains is $1/2\tau_0$. The $\theta$ dependence of the fluctuating field is given by

$$h_\perp^\pm=h_0\{\sin(\theta\pm 60°)-\sin\theta\} , \tag{16}$$

$$h_z^\pm=h_0\{\cos(\theta\pm 60°)-\cos\theta\} . \tag{17}$$

The angular dependences of $1/T_1$ and $1/T_2$ are determined only by the square $(h_\alpha^\pm)^2$ of the magnitude of field jump, although the absolute values are depend on $\tau_0$, $\tau_1$, and $\omega$. The expression of $1/T_1$ is proportional to $(h_\perp^+)^2+(h_\perp^-)^2$. The solid lines shown in Fig. 4 represent the theoretical angular dependence obtained from the best fit of Eqs. (14) and (16) to the observed values of $1/T_1$. As is seen, the theoretical curves agree well with the experimental result. The expression of $1/T_2$, on the other hand, is proportional to $(h_z^+)^2+(h_z^-)^2$, and an an-

gular dependence shifted by 90° from that of $1/T_1$ is expected. The broken line shown in Fig. 6 represents the theoretical angular dependence obtained from Eqs. (15) and (17). In this case, however, the above theory does not explain the characteristic angular dependence of $1/T_2$, that is, the value of $1/T_2$ takes a minimum value at $\theta=30°$ and 150°.

## V. ANALYSIS BY A NONLINEAR THEORY

In the above discussion we used the conventional stochastic theory of relaxation. This theory starts from the correlation function as shown in Eq. (4). This means that the relaxation rate is always proportional to the mean square $\langle \delta H^2 \rangle$ of the amplitude of the fluctuation. In our case, the theoretical angular dependence of $1/T_2$ always results in the broken line shown in Fig. 6 independent of the type of correlation function, and the observed angular dependence cannot be explained by the stochastic theory.

In the stochastic theory the fluctuation is assumed to be of the Gaussian process[29,30] or is treated as a perturbation.[31,32] The two-state pulse fluctuation here is not of Gaussian. If the pulse fluctuation cannot be treated as a perturbation in our case of transverse relaxation, it is possible that the stochastic theory is not applicable to the analysis of our experimental result.

The relaxation rates in Eqs. (2)–(4) are the result of a perturbation theory. This fact means that those are the result of a linear theory. In order to explain our experimental result of $1/T_2$, we return to the definition of transverse (or phase) relaxation and consider a nonlinear theory of phase relaxation in the pulse fluctuating field without use of the correlation function. The phase relaxation rate can be obtained directly from the relaxation function.

### A. A nonlinear theory of phase relaxation

The phase relaxation time $T_2$ is defined as the time constant of the decay of transverse magnetic moment. By considering the phase disturbance of the Larmor precession due to the longitudinal component of the fluctuation, the relaxation function $F(t)$ is written as[34]

$$F(t)=F_0\left\langle \exp\left[ i\int_0^t \delta\omega(t')dt' \right] \right\rangle , \tag{18}$$

where $\delta\omega(t)=\gamma\delta H_z(t)$, and the angular brackets $\langle\ \rangle$ denote the ensemble average. The $F(t)$ represents the amplitude of the free-induction-decay signal if inhomogeneous distribution of precession frequency were absent. When Eq. (18) is represented as

$$F(t)=F_0\exp\left[ -\frac{t}{T_2} \right] \tag{19}$$

the phase relaxation time $T_2$ can be defined.

Practically, $F(t)$ or $T_2$ is obtained by the spin-echo technique. The signal amplitude $E$ of spin echoes at $t=2\tau$ is written as[34]

$$E(2\tau)=E_0\left\langle \exp\left[ i\int_0^{\tau}\delta\omega(t)dt - i\int_{\tau}^{2\tau}\delta\omega(t)dt \right] \right\rangle , \tag{20}$$

where $\tau$ represents the time separation of the two rf pulses. Here we consider a pulse fluctuation $\delta H_z(t)$ in Fig. 9(a), which is described by random sudden jumps between two field values with field jump $h_z$ and lifetimes $\tau_0$ and $\tau_1$. The signal amplitude of spin echoes can be calculated from Eq. (20) by considering all possible pulse sequences of the fluctuation, the phase deviation [integral of $\delta\omega(t)=\gamma\delta H_z(t)$ during the time $2\tau$], and the statistical weight of the pulse sequence. The details of the calculation are given in the Appendix.

In the case of $\tau_0 \gg \tau_1$, the analytical expression of the echo amplitude becomes rather simple and is given by

$$E(2\tau)=E_0\exp\left[ -\frac{2\tau}{T_2} \right] \tag{21}$$

with

$$\Gamma_2^N(h_z)=\frac{1}{T_2}=\frac{1}{\tau_0}\frac{(\gamma h_z\tau_1)^2}{1+(\gamma h_z\tau_1)^2} . \tag{22}$$

Equation (22) is a function of the average time separation $\tau_0$ of the fluctuation pulses and the average phase jump $\gamma h_z\tau_1$ due to one fluctuation pulse. The relaxation rate is proportional to $(\gamma h_z\tau_1)^2$ when $\gamma h_z\tau_1 \ll 1$ (weak collision), while it becomes independent of $\gamma h_z\tau_1$ when $\gamma h_z\tau_1 \gg 1$ (strong collision). In the strong-collision limit, as is expected, the relaxation rate is equal to $1/\tau_0$, the number of the fluctuation pulses per unit time.

It is reasonable that the transverse relaxation rate $\Gamma_2^s(h_z)$ in Eq. (13), which is the result of the conventional stochastic theory, has the form of the weak-collision limit of our result $\Gamma_2^N(h_z)$ in Eq. (22). In the process of derivation of Eq. (22), we do not make any approximation of weak collision, and our result is valid in the whole region including both cases of weak and strong collisions.

### B. Analysis of $1/T_2$

Here we analyze the observed angular dependence of $1/T_2$ by using $\Gamma_2^N(h_z)$ in Eq. (22), which is the result of the nonlinear theory of phase relaxation, instead of $\Gamma_2^s(h_z)$ in Eq. (13). Under the spin inversion model, the transverse relaxation rate in Eq. (15) is rewritten as

$$\begin{aligned}\frac{1}{T_2}&=\frac{1}{2}\{\Gamma_2^N(h_z^+)+\Gamma_2^N(h_z^-)\}\\ &=\frac{1}{2\tau_0}\left\{ \frac{(\gamma h_z^+\tau_1)^2}{1+(\gamma h_z^+\tau_1)^2}+\frac{(\gamma h_z^-\tau_1)^2}{1+(\gamma h_z^-\tau_1)^2} \right\} .\end{aligned} \tag{23}$$

In Eq. (15) the angular dependence is determined only by $(h_z^{\pm})^2$ and is expected to be always the same independent of the other parameters. In Eq. (23) with Eq. (17), on the other hand, the angular dependence of $1/T_2$ can depend on the shorter lifetime $\tau_1$. Figure 10 shows the theoretical $\tau_1$ dependence of $1/T_2$ for each NMR line, where $1/T_2$ is normalized by $1/\tau_0$, which is the fluctuating rate of the internal field at the Cs site. The four curves correspond to the different value of $|\cos\theta|$. In the strong-collision limit ($\gamma h_0\tau_1 \gg 1$), $1/T_2$ for the $a_1$ and $a_3$ lines is a half of that for the other lines. This is because one of

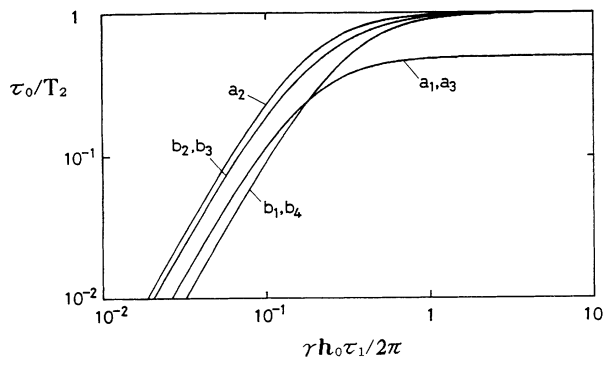


FIG. 10. Theoretical $\tau_1$ dependence of $1/T_2$ for each NMR line obtained from Eq. (23). $1/T_2$ is normalized by the fluctuating rate $1/\tau_0$ of the internal field.

the $\pm 60°$ rotations for these two lines ($\theta = 30°$ and $150°$) does not change the longitudinal field component, and then the effective number of the fluctuation pulses is reduced to one-half.

From the analysis of the observed transverse relaxation using the above calculation, we can evaluate the values of $\tau_0$ and $\tau_1$. The value of $\tau_1$ is determined by the angular dependence of $1/T_2$, or the ratios of the values of $1/T_2$, and then $\tau_0$ is determined by the absolute values of $1/T_2$. The observed angular dependence given in Fig. 6 can be explained by an intermediate collision of $\gamma h_0 \tau_1/2\pi \simeq 0.38$ in Fig. 10, which corresponds to the value of $\tau_1 \simeq 1.6\times10^{-6}$ sec. The solid line shown in Fig. 6 represents the theoretical curve obtained from the best fit to the observed values of $1/T_2$. As is seen, the theoretical calculation agrees well with the experimental result. The fitting parameters are $\tau_0 = 5.0\times10^{-4}$ sec and $\tau_1 = 1.6\times10^{-6}$ sec. These values satisfy the assumption $\tau_0 \gg \tau_1$ for Eq. (22).

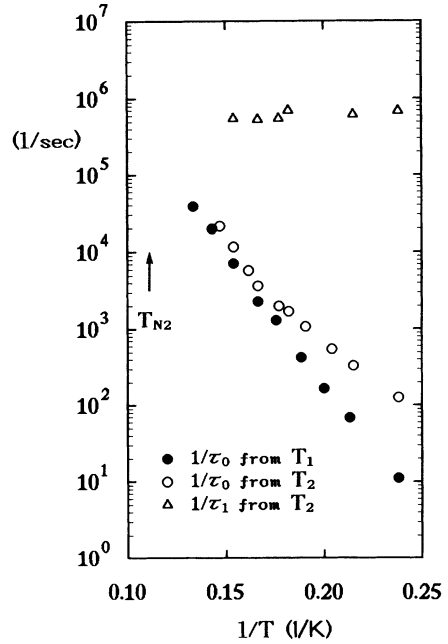


FIG. 11. Temperature dependences of the fluctuating rate $1/\tau_0$ and the inverse of the fluctuation pulse width $1/\tau_1$ of the internal field at the Cs site obtained from the $T_1$ and $T_2$ analyses.

The open circles and triangles in Fig. 11 show the temperature dependences of $1/\tau_0$ and $1/\tau_1$ obtained from the $T_2$ analysis. The fluctuating rate $1/\tau_0$ of the internal field (spin-inversion rate) exhibits remarkable increase with increasing temperature. The width of the fluctuation pulse (spin-inversion duration) $\tau_1$, on the other hand, does not exhibit appreciable change in this temperature range:

$$\tau_1 \simeq 1.6\times10^{-6} \text{ sec} . \tag{24}$$

When the external field $\mathbf{H}_0$ is applied along the $c$ axis, a single NMR line appears. The value of $T_2$ of that line was longer than that in the case of $\mathbf{H}_0$ in the $c$ plane by about one order of magnitude. This result is consistent with our model, since the rotation of the internal field in the $c$ plane gives no fluctuating-field component along $\mathbf{H}_0$.

### C. Analysis of $1/T_1$

As mentioned in Sec. IV C, the correlation time $\tau_c$ of the pulse fluctuating field in Fig. 9(a) is equal to the shorter lifetime $\tau_1$. The value of $\tau_1$ obtained from the above $T_2$ analysis is $\sim 1.6\times10^{-8}$ sec in our temperature range. In Sec. IV B, the value of $\tau_c$ has been obtained as $\sim 4\times10^{-8}$ sec from the frequency dependence of $1/T_1$ by using Eq. (8). The difference between these values is large. The longitudinal relaxation time in our experiment is much longer than the characteristic times of the fluctuation, and the effect of the fluctuation on the longitudinal relaxation can be treated as a perturbation (weak collision), although that on the transverse relaxation is not. Therefore, the use of the conventional stochastic theory for the longitudinal relaxation seems to be no problem.

To dissolve the discrepancy between the value of $\tau_c$ obtained from the frequency dependence of $1/T_1$ and that from the angular dependence of $1/T_2$, we consider that each pulse of the fluctuating field has a temporal structure of the order of $\tau_c$ as shown in Fig. 9(b). Even then the analysis of $1/T_2$ in Sec. V B is not changed. In the process of derivation of Eq. (22), we can show that the transverse relaxation rate depends only on the total pulse area or integrated phase disturbance of the fluctuation pulse but does not depend on the structure in the pulse as shown in the Appendix. We assume that $\tau_0 \gg \tau_1 \gg \tau_c$ and that the average pulse area is $h_\alpha \tau_1$ and the average pulse width is $\sim 2\tau_1$. Then the expression of the longitudinal relaxation rate $\Gamma_1^s$ of Eq. (6) or (12) is modified as

$$\Gamma_1^M(h_\perp) = \frac{2\tau_1}{\tau_0}\frac{(\gamma h_\perp)^2}{4}\frac{\tau_c}{1+(\omega\tau_c)^2} . \tag{25}$$

This expression is derived from Eq. (6) under the assumption $\tau_0 = \tau_1$ in Eq. (10) and multiplication of the duty ratio $2\tau_1/\tau_0$.

Under the spin inversion model, the longitudinal relax-

ation rate in Eq. (14) is rewritten as

$$\frac{1}{T_1}=\frac{1}{2}\{\Gamma_1^M(h_\perp^+)+\Gamma_1^M(h_\perp^-)\}$$

$$=\frac{1}{4\tau_0}\frac{\gamma^2\tau_1\tau_c}{1+(\omega\tau_c)^2}\{(h_\perp^+)^2+(h_\perp^-)^2\}\ . \tag{26}$$

The angular dependence of $1/T_1$ is the same with Eq. (14), and the observed angular dependence is well explained as shown by the solid lines in Fig. 4.

By using Eq. (26) with Eq. (16) and the evaluated values $\tau_c\simeq 4\times 10^{-8}$ sec and $\tau_1\simeq 1.6\times 10^{-6}$ sec, we can determine the value of $\tau_0$ from the observed values of $1/T_1$. The solid circles in Fig. 11 show the temperature dependence of the spin-inversion rate $1/\tau_0$ obtained from the experimental result of $1/T_1$ by using Eq. (26). The value of $1/\tau_0$ obtained from $1/T_1$ agrees well with that for $1/T_2$, although the agreement is not good in the lower temperature region. This disagreement may be caused by the fact that the transverse relaxation rate can be affected by the nuclear dipole interaction between the Cs nucleus and the surrounding nuclei Cs, Cl, or Co. The effect of this interaction may appear in the lower temperature region where the transverse relaxation rate due to the spin inversion becomes small.

In the external field $\mathbf{H}_0\|\mathbf{c}$, as mentioned in the preceding section, the value of $T_2$ was longer than that in the case of $\mathbf{H}_0\perp\mathbf{c}$ by about one order of magnitude in the higher temperature region. In the lower temperature region, however, the slope of the temperature dependence of $1/T_2$ became small remarkably, and the value of $1/T_2$ became of the same order of magnitude as that in the case of $\mathbf{H}_0\perp\mathbf{c}$. This fact supports the appearance of the effect of the nuclear dipole interaction.

Although the quantitative estimate of the effect of the nuclear dipole interaction on the transverse relaxation rate is not easy, its upper limit can be calculated by using the method of second moment.[35] We calculated the second moment $\langle\Delta\omega^2\rangle$ due to the nuclear dipole interactions between the Cs nucleus and the surrounding nuclei and obtained $(\langle\Delta\omega^2\rangle)^{1/2}\sim 10^3\ \mathrm{sec}^{-1}$, which gives an estimate of the linewidth or the decay rate of free induction decay. The transverse relaxation rate due to nuclear dipole interaction measured by spin echoes is not larger than the value of $(\langle\Delta\omega^2\rangle)^{1/2}$, and this value gives the upper limit of the transverse relaxation rate. The low-temperature disagreement in $\tau_0$ between the $T_1$ and the $T_2$ analyses suggests the additional rate of $\sim 10^2\ \mathrm{sec}^{-1}$ due to the effect of the nuclear dipole interactions on $1/T_2$. This value suggested by the experiment is not inconsistent with the above calculation of the second moment.

## VI. DISCUSSION

As shown by the analyses in the above, our experimental results of $1/T_1$ and $1/T_2$ can be explained consistently by the pulselike fluctuation in Fig. 9(b) due to the spin inversion in the $Co^{2+}$ chain. At the Cs site, the fluctuation pulse appears at the rate of $1/\tau_0$, and each pulse has an average total width $\sim 2\tau_1$ and a temporal structure of the order of $\tau_c$. (The factor 2 of the width is not essential, but the average pulse area $h_\alpha\tau_1$ is important.) The value of $\tau_0$ exhibits remarkable temperature dependence, while the values of $\tau_1$ and $\tau_c$ do not exhibit appreciable change.

The spin dynamics in the $Co^{2+}$ chain deduced from the pulselike fluctuation at the Cs site is as follows. The $Co^{2+}$ spins, which lies in the ferrimagnetic stable directions, are inverted locally in the chain for a short time. This type of spin inversion is a characteristic magnetic excitation in the Ising spin system. The magnetic excitation is created thermally at the rate of $1/\tau_0$, and the rate increases exponentially as the temperature is increased. The magnetic excitation moves back and forth in the linear chain with a characteristic time $\tau_c$ and is annihilated spontaneously with a lifetime of the order of $\tau_1$. Then the temperature dependent $\tau_0$ and the temperature independent $\tau_1$ and $\tau_c$ are well explained. This interpretation strongly suggests domain-wall pairing in the $Co^{2+}$ chain.

Pair states and bound states of domain walls were discussed theoretically by Matsubara and Inawashiro.[23,24] In their model the pairing of domain walls is caused by a weak next-nearest-neighbor interaction in the linear chain. Although we do not think that their theory, as it is, can apply to our case of 3D ordered phase, we suppose that the domain walls are weakly coupled through the interchain interaction $J_2$ and move in a form of pair, and that individual domain wall moves rather randomly keeping an appropriate distance with its partner. The spin inversion in the 3D ordered phase has no energy loss due to the nearest-neighbor antiferromagnetic interchain interactions ($J_1$), while it has a energy loss due to the next-nearest-neighbor ferromagnetic interchain interactions ($J_2$). Therefore, the length of the region between two domain walls, where the $Co^{2+}$ spins are inverted, will not be so large at the low temperatures. In thermal equilibrium the number $N$ of spins in an inverted region expected from the value of $J_2$ (Ref. 18) is of the order of $10^2$ in our temperature range, if we assume that the energy loss due to the interaction with six next-nearest-neighbor chains is of the order of $kT$ ($6J_2N\simeq kT$).

The values of $\tau_0$ and $\tau_1$ near the temperature $T_{N2}$ could not be obtained from our experiments. In Fig. 11, however, it seems that the value of $\tau_0$ becomes of the same order of magnitude as the value of $\tau_1$ at $T_{N2}$. It may be reasonable to consider that the phase transition at $T_{N2}$ occurs when the lifetime $\tau_0$ of the stable state becomes comparable with the spin-inverted duration $\tau_1$, since the ferrimagnetic stable state is no longer stable on that occasion.

Our experimental results were well explained by the spin inversion model; the spin-inversion duration $\tau_1$ is much shorter than the lifetime $\tau_0$ of the stable state. This type of spin inversion ($\tau_0\gg\tau_1$) is a characteristic spin dynamics in the 3D ordered phase, and is different from that caused by the propagation of free solitons ($\tau_0=\tau_1$)[12] in the intermediate and the paramagnetic phases. Here we examine the possibility of taking the model of free soliton propagation. Since the pulse fluctuation in Fig. 9(a)

with $\tau_0=\tau_1$ is expected in this case, the longitudinal relaxation rate is given by Eqs. (6) and (10) as

$$\Gamma_1^s(h_\perp)=\frac{(\gamma h_\perp)^2}{4}\frac{\tau_c}{1+(\omega\tau_c)^2}\ , \tag{27}$$

where $\tau_c=\tau_0/2=\tau_1/2$. This rate is expressed by a single characteristic time $\tau_c$. The value of $\tau_c$ is expected to have a remarkable temperature dependence due to the change of soliton density. Therefore, the free soliton model does not explain the temperature-independent value of $\tau_c$ obtained from the frequency dependence of $1/T_1$ in our experiment. Similar discrepancy can be shown for the temperature-independent angular dependence of $1/T_2$.

## VII. SUMMARY

We measured the longitudinal relaxation time $T_1$ and the transverse relaxation time $T_2$ of $^{133}$Cs NMR in the low-temperature phase of $CsCoCl_3$. The relaxation rates $1/T_1$ and $1/T_2$ exhibit characteristic angular dependences and remarkable temperature dependences. The longitudinal relaxation rate exhibits NMR-frequency dependence, while the transverse relaxation rate does not.

From an analysis of fluctuating internal field at the Cs nuclei by using the spin inversion model, the experimental results were interpreted in terms of a pulselike fluctuation; the pulselike fluctuation at the Cs site appear at the rate $1/\tau_0$, and each pulse has an average total width $\sim 2\tau_1$ including a rapid fluctuation of the order of $\tau_c$. The experimental results of $1/T_1$ and $1/T_2$ were consistently explained by this model. These facts suggest that the domain walls exist in a form of pair and move back and forth in the $Co^{2+}$ chain.

We analyzed the experimental results by using the stochastic theory. The temperature-independent value of the correlation time $\tau_c$ was obtained from the frequency dependence of $1/T_1$ as $\tau_c\simeq 4\times 10^{-8}$, and the angular dependence of $1/T_1$ was well explained by the spin inversion model. The angular dependence of $1/T_2$, however, could not be explained by the conventional stochastic theory, which is valid only for the case of the weak-collision limit. We developed a nonlinear theory of phase relaxation in the pulse fluctuating field, which is valid for general cases including the weak- and strong-collision limits; the transverse relaxation rate was calculated by considering the phase disturbance of the Larmor precession due to the fluctuating internal field. Then the angular dependence of $1/T_2$ was well explained. The spin-inversion duration $\tau_1$ was obtained from the angular dependence of $1/T_2$, and then the value of spin-inversion rate $1/\tau_0$ was obtained from the absolute values of $1/T_2$. The value of $1/\tau_0$ was obtained also from the analysis of $1/T_1$, and agreed with that from the analysis of $1/T_2$.

It was found that the spin-inversion rate exhibits remarkable temperature dependence, while the correlation time and the spin-inversion duration does not change appreciably in our temperature range. From the dynamical point of view, the phase-transition point at $T_{N2}$ can be explained as a point where the ferrimagnetic stable state is no longer stable; the lifetime $\tau_0$ of the stable state becomes comparable with the spin-inverted duration $\tau_1$ at the temperature $T_{N2}$.

## APPENDIX: A NONLINEAR THEORY OF PHASE RELAXATION IN A PULSE FLUCTUATING FIELD

The experimental result of $1/T_2$ could not be explained by the stochastic theory as shown in Sec. IV. This may be caused by the fact that the conventional stochastic theory is valid only for the case of weak collision. In order to explain our experimental result, we consider a nonlinear theory of phase relaxation. The phase relaxation time $T_2$ is defined as the time constant of the decay of transverse magnetic moment. We directly calculate the signal amplitudes of free induction decay (FID) and spin echoes in Eqs. (18) and (20) by considering the phase disturbance of the Larmor precession due to the longitudinal fluctuation, and derive the phase relaxation rate, which is valid for general cases.

Here we consider the two-state pulse fluctuating field $\delta H_z(t)$ in Fig. 9(a), which is described by random sudden jumps between two field values with field jump $h_z$ and lifetimes $\tau_0$ and $\tau_1$. We assume that $\tau_0\gg\tau_1$, the $k$th fluctuation pulse appears at time $t_k$, and its pulse width is $u_k$.

The signal amplitudes of FID and spin echoes can be calculated from Eqs. (18) and (20) by considering all possible pulse sequences of the fluctuation, the phase deviation, and the statistical weight of the pulse sequence. To calculate the ensemble average we introduce an averaging operator $\hat{p}_T(t)$;

$$\hat{p}_T(t)=\sum_{n=0}^{\infty}\hat{p}_n(t)\ . \tag{A1}$$

This operator is similar to that of Hu and Hartmann[36] but not the same. The operator $\hat{p}_n(t)$, which is referred to as the $n$th averaging operator, averages some quantity for all possible pulse sequences of duration $t$ composed of $n$ fluctuation pulses. The $n$th averaging operator is given by

$$\hat{p}_n(t)=\int_0^t dt_1\int_0^t du_1\int_{t_1}^t dt_2\int_0^t du_2\cdots\int_{t_{n-1}}^t dt_n\int_0^t du_n q_n(t;u_1,\ldots,u_n)\ , \tag{A2}$$

where $q_n(t;u_1,\ldots,u_n)$ represents the statistical weight of the pulse sequence. The probability that the field value jumps up in the time interval between $t_k$ and $t_k+dt_k$ and jumps down in the interval between $t_k+u_k$ and $t_k+u_k+du_k$ $(k=1,\ldots,n;\ t_{n+1}=t)$ is given by

$$q_n(t;u_1,\ldots,u_n)dt_1du_1\cdots dt_ndu_n=\exp\left[-\frac{t_1}{\tau_0}\right]\prod_{k=1}^{n}\frac{dt_k}{\tau_0}\exp\left[-\frac{u_k}{\tau_1}\right]\frac{du_k}{\tau_1}\exp\left[-\frac{t_{k+1}-t_k}{\tau_0}\right]$$

$$=\exp\left[-\frac{t}{\tau_0}\right]\frac{1}{(\tau_0\tau_1)^n}\prod_{k=1}^{n}dt_k du_k\exp\left[-\frac{u_k}{\tau_1}\right], \tag{A3}$$

where we assumed that at time 0 or $t$ the fluctuating field is in the lower state whose lifetime is $\tau_0$. This is reasonable because, in the case of $\tau_0\gg\tau_1$, the statistical weight that the fluctuation field is in the upper state at those times is negligible.

Before calculation of the phase relaxation rate, we examine the probability that $n$ fluctuation pulses appear during a time interval $t$. This probability is given by $\hat{p}_n(t)\cdot 1$ and obtained from Eqs. (A2) and (A3);

$$\hat{p}_n(t)\cdot 1\simeq\exp\left[-\frac{t}{\tau_0}\right]\frac{1}{(\tau_0\tau_1)^n}\left[\int_0^t dt\right]^n\frac{1}{n!}\left\{\int_0^\infty du\exp\left[-\frac{u}{\tau_1}\right]\right\}^n$$

$$=\frac{1}{n!}\left[\frac{t}{\tau_0}\right]^n\exp\left[-\frac{t}{\tau_0}\right]. \tag{A4}$$

This means that the number of the fluctuation pulse is described by the Poisson distribution with an average number $\bar{n}=t/\tau_0$. The sum of all probability, of course, becomes unity:

$$\hat{p}_T(t)\cdot 1=\sum_{n=0}^{\infty}\hat{p}_n(t)\cdot 1=\left\{\sum_{n=0}^{\infty}\frac{1}{n!}\left[\frac{t}{\tau_0}\right]^n\right\}\exp\left[-\frac{t}{\tau_0}\right]=1. \tag{A5}$$

Using the averaging operator the signal amplitudes of FID and spin echoes in Eqs. (18) and (20) are written as

$$F(t)=F_0\hat{p}_T(t)\exp\left[i\gamma\int_0^t\delta H_z(t')dt'\right]=F_0\sum_{n=0}^{\infty}\langle f_n(t,+)\rangle, \tag{A6}$$

$$E(2\tau)=E_0\hat{p}_T(2\tau)\exp\left[i\gamma\int_0^\tau\delta H_z(t)dt-i\gamma\int_\tau^{2\tau}\delta H_z(t)dt\right]=E_0\sum_{m=0}^{\infty}\sum_{n=0}^{\infty}\langle f_m(\tau,+)\rangle\langle f_n(\tau,-)\rangle, \tag{A7}$$

where $\langle f_n(t,\pm)\rangle$, which is referred to as the $n$th averaged phase factor, represents the contribution to the averaged phase factor of the pulse sequences with $n$ fluctuation pulses during the time interval $t$. Since the phase deviation due to the $k$th pulse is $\gamma h_z u_k$, the $n$th averaged phase factor is defined as

$$\langle f_n(t,\pm)\rangle=\hat{p}_n(t)\exp\left[\pm i\gamma h_z\sum_{k=1}^{n}u_k\right]. \tag{A8}$$

The $n$th averaged phase factor can be expressed by an analytical form using the $n$th averaging operator in Eqs. (A2) and (A3) and given by

$$\langle f_n(t,\pm)\rangle\simeq\exp\left[-\frac{t}{\tau_0}\right]\frac{1}{(\tau_0\tau_1)^n}\left[\int_0^t dt\right]^n\frac{1}{n!}\left\{\int_0^t du\exp\left[\left[-\frac{1}{\tau_1}\pm i\gamma h_z\right]u\right]\right\}^n$$

$$\simeq\exp\left[-\frac{t}{\tau_0}\right]\frac{1}{n!}\left\{\frac{t}{\tau_0\tau_1}\int_0^\infty du\exp\left[\left[-\frac{1}{\tau_1}\pm i\gamma h_z\right]u\right]\right\}^n. \tag{A9}$$

In the above we assumed a two-state pulse type of fluctuation with average pulse width $\tau_1$. The derivation of phase relaxation rate, however, does not depend on the shape of the pulse. The average pulse area $h_z\tau_1$ is important for the phase relaxation, and the result is independent of the temporal structure in a pulse if the effective value of the average pulse width is described by a lifetime $\tau_1$;

$$\left\langle\int_{\text{pulse}}\delta H_z(t)dt\right\rangle=h_z\tau_1. \tag{A10}$$

The longitudinal relaxation rate, on the other hand, depend on the temporal structure in a pulse. This corresponds to the fact that the longitudinal relaxation rate is determined by the $\omega$ component $G_\perp(\omega)$ and the transverse relaxation rate is determined by the low-frequency component $G_z(0)$ as shown in Eqs. (2)–(4) in Sec. IV.

The signal amplitudes of FID and spin echoes can be obtained from Eqs. (A6), (A7), and (A9). Its analytical expression becomes rather simple and given by

$$F(t)=F_0\exp\left[-\frac{t}{\tau_0}\right]\exp\left\{\frac{t}{\tau_0\tau_1}\int_0^\infty du\exp\left[\left[-\frac{1}{\tau_1}+i\gamma h_z\right]u\right]\right\}=F_0\exp\left[-\frac{t}{T_2}+i\Delta\omega t\right], \tag{A11}$$

$$E(2\tau)=E_0\exp\left[-\frac{2\tau}{\tau_0}\right]\exp\left\{\frac{2\tau}{\tau_0\tau_1}\int_0^\infty du\exp\left[-\frac{u}{\tau_1}\right]\cos(\gamma h_z u)\right\}=E_0\exp\left[-\frac{2\tau}{T_2}\right], \tag{A12}$$

with

$$\frac{1}{T_2}=\frac{1}{\tau_0}\frac{(\gamma h_z\tau_1)^2}{1+(\gamma h_z\tau_1)^2}, \tag{A13}$$

$$\Delta\omega=\frac{1}{\tau_0}\frac{\gamma h_z\tau_1}{1+(\gamma h_z\tau_1)^2}. \tag{A14}$$

Equations (A13) and (A14) give the phase relaxation rate $1/T_2$ and the frequency shift $\Delta\omega$, respectively. The decay curves of the phase relaxation measured by FID and spin echoes are single exponential and their relaxation rates are the same in the case of the pulse fluctuating field. The phase relaxation rate in Eq. (A13) well explains our experimental result of $1/T_2$.


[1]N. Achiwa, J. Phys. Soc. Jpn. **27**, 561 (1969).
[2]U. Tellenbach and H. Arend, J. Phys. C **10**, 1311 (1977).
[3]H. Yoshizawa and K. Hirakawa, J. Phys. Soc. Jpn. **46**, 448 (1979).
[4]H. Yoshizawa, K. Hirakawa, S. K. Satija, and G. Shirane, Phys. Rev. B **23**, 2298 (1981).
[5]S. E. Nagler, W. J. L. Buyers, R. L. Armstrong, and B. Briat, Phys. Rev. B **27**, 1784 (1983).
[6]J. P. Boucher, L. P. Regnault, J. Rossat-Mignod, Y. Henry, J. Bouillot, and W. G. Stirling, Phys. Rev. B **31**, 3015 (1985).
[7]K. Adachi, J. Phys. Soc. Jpn. **50**, 3904 (1981).
[8]J. P. Boucher, G. Rius, and Y. Henry, Europhys. Lett. **4**, 1073 (1987).
[9]H. Kikuchi and Y. Ajiro, J. Phys. Soc. Jpn. **58**, 2531 (1989).
[10]K. Adachi, M. Hamashima, Y. Ajiro, and M. Mekata, J. Phys. Soc. Jpn. **47**, 780 (1979).
[11]Y. Ajiro, H. Kikuchi, T. Okita, M. Chiba, K. Adachi, M. Mekata, and T. Goto, J. Phys. Soc. Jpn. **58**, 390 (1989).
[12]H. Kikuchi and Y. Ajiro, J. Phys. Soc. Jpn. **58**, 692 (1989).
[13]W. P. Lehmann, W. Breitling, and R. Weber, J. Phys. C **14**, 4655 (1981).
[14]I. Mogi, N. Kojima, Y. Ajiro, H. Kikuchi, T. Ban, and I. Tsujikawa, J. Phys. Soc. Jpn. **56**, 4592 (1987).
[15]J. Villain, Physica **79B**, 1 (1975).
[16]M. Mekata, J. Phys. Soc. Jpn. **42**, 76 (1977).
[17]N. Ishimura and H. Shiba, Prog. Theor. Phys. **63**, 743 (1980).
[18]H. Shiba, Prog. Theor. Phys. **64**, 466 (1980).
[19]K. Maki, Phys. Rev. B **24**, 335 (1981).
[20]H. Shiba and K. Adachi, J. Phys. Soc. Jpn. **50**, 3278 (1981).
[21]F. Matsubara and S. Ikeda, Phys. Rev. B **28**, 4064 (1983).
[22]F. Matsubara and S. Inawashiro, Phys. Rev. B **41**, 2284 (1990).
[23]F. Matsubara and S. Inawashiro, J. Phys. Soc. Jpn. **58**, 4284 (1989).
[24]F. Matsubara and S. Inawashiro, Phys. Rev. B **43**, 796 (1991).
[25]J. A. Holyst, Z. Phys. B **74**, 341 (1989).
[26]J. A. Holyst and H. Benner, Solid State Commun. **72**, 385 (1989).
[27]H. Benner, J. A. Holyst, and J. Löw, Europhys. Lett. **14**, 383 (1991).
[28]T. Kohmoto, T. Goto, S. Maegawa, N. Fujiwara, Y. Fukuda, M. Kunitomo, and M. Mekata, Phys. Lett. A **167**, 493 (1992).
[29]R. Kubo, in *Fluctuations, Relaxation and Resonance in Magnetic Systems,* edited by D. ter Haar (Oliver and Boyd, Edinburgh, 1962), p. 23.
[30]R. Kubo, M. Toda, and N. Hashitsume, *Statistical Physics II Nonequilibrium Statistical Mechanics* (Springer-Verlag, Berlin, 1991), p. 40.
[31]C. P. Slichter, *Principles of Magnetic Resonance* (Springer-Verlag, Berlin, 1989), p. 206.
[32]F. Borsa, in *Local Properties at Phase Transitions,* edited by K. A. Müler and A. Rigamonti (North-Holland, Amsterdam, 1976), p. 137.
[33]G. E. G. Hardeman, N. J. Poulis, and W. Van der Lugt, Physica **22**, 48 (1956).
[34]J. R. Klauder and P. W. Anderson, Phys. Rev. **125**, 912 (1962).
[35]C. P. Slichter, *Principles of Magnetic Resonance* (Springer-Verlag, Berlin, 1989), p. 71.
[36]P. Hu and S. R. Hartmann, Phys. Rev. B **9**, 1 (1974).